

Nonlinear Collisionless Magnetic Reconnection

M Ottaviani, F Porcelli.

JET Joint Undertaking, Abingdon, Oxon, OX14 3EA.

"This document is intended for publication in the open literature. It is made available on the understanding that it may not be further circulated and extracts may not be published prior to publication of the original, without the consent of the Publications Officer, JET Joint Undertaking, Abingdon, Oxon, OX14 3EA, UK".

"Enquiries about Copyright and reproduction should be addressed to the Publications Officer, JET Joint Undertaking, Abingdon, Oxon, OX14 3EA".

Nonlinear Collisionless Magnetic Reconnection

M Ottaviani, F Porcelli.

JET Joint Undertaking, Abingdon, Oxfordshire, OX14 3EA, UK.

INTRODUCTION.

Magnetic reconnection in collisionless regimes, where electron inertia is responsible for the decoupling of the plasma motion from that of the magnetic field, is a well known process in Astrophysics¹. Recently this process has also been observed in tokamak plasmas. Specifically, at the high plasma temperatures reached in JET, sawteeth commonly occur on a time scale shorter than the electron-ion collision time. These observations have initially motivated the extension of the linear theory of $m=1$ kink-tearing modes to the experimentally relevant regimes³⁻⁶, leading to the conclusion that these modes can remain virulent at low collisionality with an initial growth rate which compares favourably with that observed in the experiments. However, the nonlinear evolution has remained unclear. While Wesson's⁷ modification of the Sweet-Parker-Kadomtsev⁸⁻¹⁰ scaling has given an estimate of the collisionless reconnection time in good agreement with that observed experimentally, Drake&Kleva's numerical simulation¹¹ of the merging of two isolated flux bundles has led to the suggestion that the collisionless reconnection rate is greatly reduced as the nonlinear phase is entered, i.e. for magnetic island widths comparable with the plasma skin depth.

In order to clarify these issues, we analyze the behavior of *a collisionless, incompressible 2-D slab model where Larmor radius effects are neglected*. The main result of our numerical and analytic investigation is that when the island size is larger than the linear layer but smaller than the macroscopic (equilibrium) scale length *the system evolves faster than exponentially*.

THE MODEL.

$$\partial_t U + [\varphi, U] = [J, \psi] \quad \text{vorticity equation} \quad (1)$$

$$\partial_t F + [\varphi, F] = 0 \quad \text{collisionless Ohm's law} \quad (2)$$

where $[A, B] \equiv \mathbf{e}_z \cdot \nabla A \times \nabla B$, with \mathbf{e}_z the unit vector along the z direction. $U = \nabla^2 \varphi$ is the fluid vorticity, φ is the stream function, $\mathbf{v} = \mathbf{e}_z \times \nabla \varphi$ is the fluid velocity, $J = -\nabla^2 \psi$ is the current density along z , ψ is the magnetic

flux function and $F \equiv \psi + d^2 J$, with d the skin depth. Thus, $[\phi, F] = \mathbf{v} \cdot \nabla F$ and the collisionless Ohm law (2) can be written as $dF/dt = 0$.

Key point: F is conserved on a moving fluid element.

Boundary Conditions and normalizations: The co-ordinate z is ignorable, $\partial_z = 0$. The co-ordinates x and y vary in the intervals $x \in [-L_x, L_x]$ and $y \in [-L_y, L_y]$, with the slab aspect ratio $\epsilon \equiv L_x/L_y < 1$. Periodic boundary conditions are imposed at the edge of these intervals. The magnetic field is $\mathbf{B} = B_0 \mathbf{e}_z + \nabla \psi \times \mathbf{e}_z$, with a constant B_0 . All quantities in Eqs. (1,2) are dimensionless, with $L_x = \pi$ and $\tau_A = (4\pi\rho_m)^{1/2} L_x / B_0$ determining the length and time scale normalisation.

Equilibrium: $\phi_0 = U_0 = 0$, $J_0 = \psi_0 = \cos x$, and $F_0 = (1 + d^2)\psi_0$.

Initial Conditions: A small tearing-type linear perturbations of the form $(\phi, \delta\psi) = \text{Real}\{[\phi_L(x), \delta\psi_L(x)]e^{\gamma t + iky}\}$ is added to the equilibrium to construct the initial conditions. Here $k = m\epsilon$, with m an integer number. In the limit $d \ll L_x$, the solution of the linearized system can be obtained analytically using asymptotic matching techniques. For $0 < k^2 \leq 1$ the logarithmic jump of $\delta\psi_L$ across the reconnecting layers is $\Delta' = 2\kappa \tan(\kappa\pi/2)$, with $\kappa \equiv (1 - k^2)^{1/2}$.

Regime of interest: the *large- Δ'* regime, defined by

$$\Delta' d \geq 1 \quad \Rightarrow \quad \text{Macroscopic convective cells} \quad (3)$$

satisfied for low values of m and $\epsilon^2 \ll 1$ such that $\Delta' \sim (8/\pi k^2)$. In this regime, *the structure of the stream function is macroscopic*, with $\phi_L \approx \phi_\infty \text{sign } x$, $\phi_\infty \equiv (\gamma/k)\psi_\infty$, everywhere except in narrow layers near the reconnecting surfaces. Here we choose $\epsilon = 0.5$ (to ensure that only $m = 1$ is unstable) and $d/(2L_x) = 0.04$, which gives $d\Delta' \approx 2.03$ thus satisfying condition (3). The current channel in the linear stage has a width $\delta_L \sim d$. The linear growth rate is $\gamma_L \approx kd$.

NUMERICAL SOLUTION.

The model equations are solved with a pseudospectral code¹² advancing in time the Fourier representation of the field variables, truncated to 1024x64 (x, y) components.

Regime of interest: the early nonlinear phase, defined by the condition $d < w < 2L_x$, where w is the magnetic island width.

An important consequence of Ohm's law and of the initial conditions is that the value of F on the rational surface $x = 0$ is frozen to its initial value, i.e. $F(x = 0, y, t) = F_0(x = 0) = 1 + d^2$.

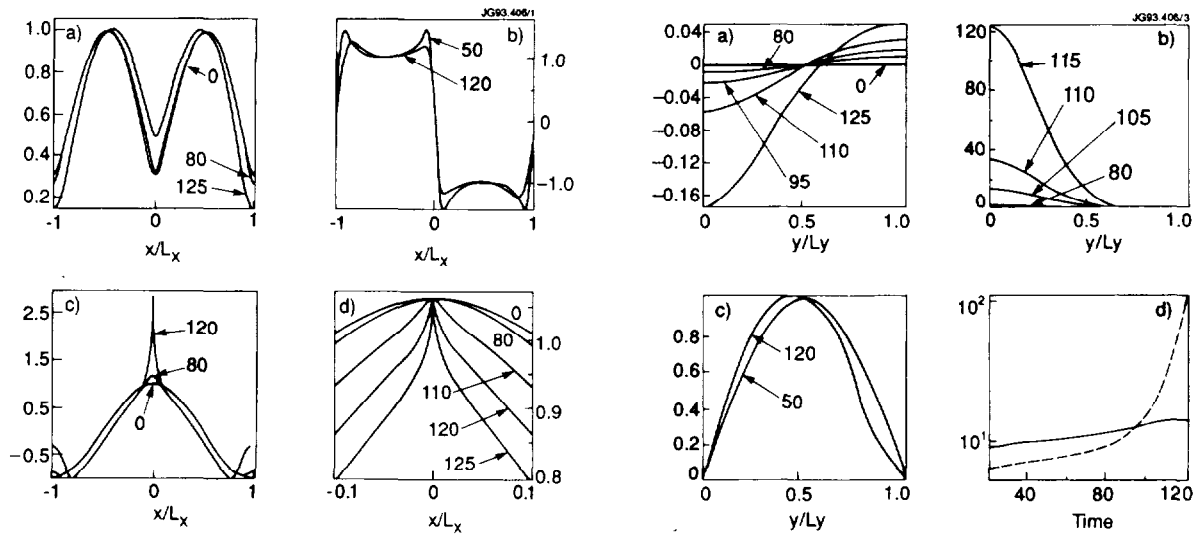


Fig. 1. Cross sections of a) $\delta\psi \equiv \psi - \psi_0$; b) $v_x = -\partial\phi/\partial y$; c) J and d) F across the X-point ($y = 0$) at various times, indicated by arrows.

Fig. 2. Cross sections of a) $\delta\psi \equiv \psi - \psi_0$; b) $\partial^2 F / \partial x^2$; c) $v_y / (v_y)_{y=L_y/2}$ along the reconnection line ($x = 0$) at various times indicated by arrows. Also, d) time dependence of the logarithm of the inverse of the profile widths $\delta_\phi \equiv (v_x)_{x=L_x/2} / (\partial_x v_x)_{x=0}$ (solid line) and $\delta_J \equiv (\partial_x^2 \delta J / \delta J)^{-1/2} < d$ (broken line).

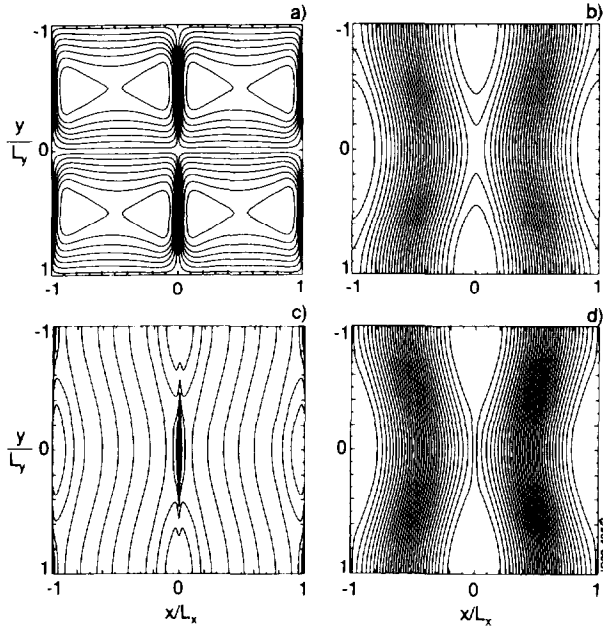


Fig. 3. Contour plots at $t=120$: a) ϕ ; b) ψ ; c) J ; d) F .

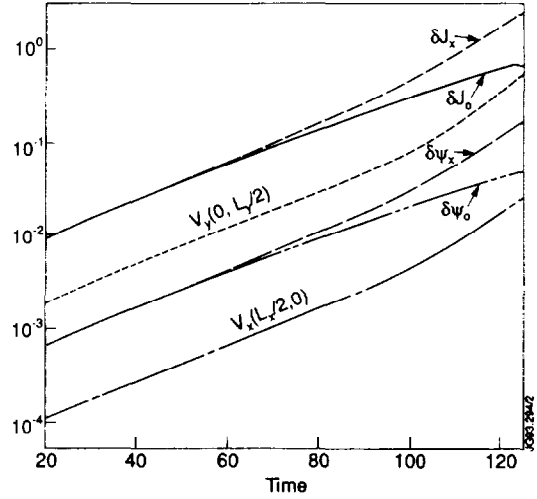


Fig. 4. Time dependence of $\delta\psi$ and δJ at the X- and O-points, of $v_x(-L_x/2, 0)$ and of $v_y(0, L_y/2)$.

RELEVANT PHENOMENOLOGY.

- The linear phase conventionally lasts until $t \sim 80$, when the magnetic island reaches a width of order d .
- For $t > 80$, the width of the profile of v_x , as well as that of $\delta\psi$, remains of the order of the skin depth (Figs. 1a,b and Fig. 2d). The convection cells retain approximately their linear shape well into the nonlinear phase (Fig. 3a).
- By contrast, the current density profile (Fig. 1c) develops a sub-layer whose width around the X-point, keeps shrinking with time (see also Fig. 2d). This sub-layer is also visible in the profile of F across the X-point (Fig. 1d).
- The contraction of this sub-layer is extremely rapid in time, as shown also by the graph of $\partial^2 F / \partial x^2$ versus y for $x = 0$ (Fig. 2b). The simulation is stopped when this layer has become so narrow that it can no longer be resolved by our truncated Fourier expansion.
- Note the development of a current sheet around the reconnection line (Fig. 3c).
- Also note the preservation of the topology of the isolines of F (Fig. 3d).
- Finally (Fig. 4) the mode growth remains very rapid throughout the simulation. Indeed, the growth rate of ϕ , as well as that of $\delta\psi$ and δJ at the X-points, accelerate in the early nonlinear phase, which is symptomatic of an explosive behaviour (the mode growth slows down only when the island size approaches the macroscopic scale length L_x).

ANALYTIC TREATMENT.

The fact that the spatial structure of the stream function does not vary significantly with time throughout the linear and early nonlinear phases suggests the *ansatz*:

$$\varphi(x, y, t) = v_o(t)g(x)h(y) + u(x, y, t) \quad (4)$$

where $h(y) \sim k^{-1} \sin(ky)$, $g(x) \sim \varphi_L(x)/\varphi_\infty$ contains the linear scale length d and $u(x, y, t)$ develops the rapid scale length $\delta(t) \sim \delta_J$ observed in the numerical simulation.

Assume $u \ll v_o$ and $\partial_x u \sim v_o \partial_x g$. These assumptions allow an analytic treatment of the system of Eqs. (1,2).

- Integrate the collisionless Ohm's law (2) with the method of the characteristics. This yields $F = F_o(x_o)$, where $x_o(x, y, t) = x - \xi(x, y, t)$ is the initial position of a fluid element situated at (x, y) at time t and ξ is the displacement along the x direction defined by the equation $d\xi/dt = v_x$, $\xi(t = -\infty) = 0$. *The ansatz (4) allows one to neglect $u(x, y, t)$. One finds:*

$$-\int_{x_o}^x dx'/g(x') = \int_{-\infty}^t v_o(t') dt' \equiv \lambda(t). \quad (5)$$

where the function $\lambda(t) > 0$ represents the amplitude of ξ outside the reconnection layer, where $g(x) \approx 1$. In the linear phase, $-\psi_\infty \approx \lambda < d$. When $\lambda > d$, the magnetic island width $w \sim 2\lambda$, so that the early nonlinear phase can also be characterised by the inequality $d < \lambda < L_x$, or alternatively $t_0 < t < t_D$, with $\lambda(t_0) \sim d$ and t_D the characteristic turnover time of the macroscopic eddies in Fig. 3a.

- Invert Equation (5) to obtain $x_o = x_o(x, t)$. In the limit $d < \lambda < L_x$, the new time-dependent scale length appears:

$$\delta(t) \equiv d \exp[-\lambda(t)/d], \quad (6)$$

such that x_o has the following behaviour around $y = 0$:

$$\begin{aligned} x_o &\sim (x/\delta) \hat{d} && \text{for } |x| < \delta; \\ x_o &\sim \left[\lambda + \hat{d} \ln(|x|/\hat{d}) \right] \text{sign}(x) && \text{for } d > |x| > \delta \\ x_o &\sim \lambda \text{sign}(x) + x && \text{for } |x| > d \end{aligned}$$

where $\hat{d} \equiv (dg/dx)_{x=0}^{-1} \sim d$. Thus we see that near the X-point along the x direction, $F(x_0)$ (and hence J) varies over a distance $\delta(t)$ which becomes exponentially small in the ratio λ/d . Conversely, around the O-point F flattens over a distance $|x| \sim \lambda$.

Physical meaning: The formation of a sub-layer is the combined result of the conservation of F on each fluid element and the (hyperbolic) flow pattern around the X-point, which acts to increase the local curvature of the F profile (Fig. 1d).

- Obtain ψ by integrating the equation $\psi + d^2 J = F$ (see appendix A1). Asymptotic evaluation of ψ at the X- and O-points in the early nonlinear phase ($\lambda > d$) gives

$$\psi_x \equiv \psi(0,0,t) \sim 1 - \frac{1}{2} \lambda^2(t), \quad \psi_o \equiv \psi(0, \pm L_y, t) \sim 1 + (d^2) \quad (7)$$

Key point: an asymmetry develops in the values of $\delta\psi$ and of J between the X- and O-points. The spike of the current density at the X-point has an amplitude $\delta J_x \sim 0.5(\lambda/d)^2$.

- Integrate the vorticity equation (1) over the quadrant $S: [0 \leq x \leq L_x, 0 \leq y \leq L_y]$, such that $\int_S [\phi, U] dx dy = 0$.

$$\partial_t \int_S U dx dy = \oint_C J d\psi. \quad (8)$$

where C is the boundary of S . The dominant contribution to the l.h.s. comes from v_y (appendix A2):

$$\partial_t \int_S U dx dy \approx -\frac{1}{d} d^2 \lambda / dt^2. \quad (9)$$

The dominant contribution from the r.h.s. of Eq. (8) can be evaluated exactly (appendix A2):

$$\oint_C J d\psi \approx \delta\psi_x - \delta\psi_o - (\delta\psi_x^2 - \delta\psi_o^2) / 2d^2. \quad (10)$$

- Finally, Use an interpolation formula between the linear and early nonlinear limits of the r.h.s. of (10), to obtain an equation for the evolution of $\hat{\lambda}(t) \equiv \lambda(t)/d$:

$$d^2 \hat{\lambda} / d\hat{t}^2 \approx \hat{\lambda} + c \hat{\lambda}^4; \quad c > 0 \quad (11)$$

where $\hat{t} \equiv \gamma_L t$ and c can be taken constant. The solution is $\hat{\lambda}(\hat{t}) = \left[(1-\alpha) / (1-\alpha e^{3\hat{t}}) \right]^{2/3} e^{\hat{t}}$, where $\alpha = \beta - (\beta^2 - 1)^{1/2}$, $\beta = 1 + 5/c$, and we have chosen the time origin so that $\hat{\lambda}(0) \equiv 1$. Thus, *once the early nonlinear regime is entered, $\lambda(t)$ accelerates and reaches a macroscopic size over a fraction $\sim \ln(\alpha^{-1/3})$ of the linear growth time.* Eventually, we can expect this quasi-explosive growth to cease as λ approaches L_x .

CONCLUSIONS.

- A collisionless, incompressible 2-D slab model of magnetic reconnection has been investigated with numerical and analytic methods, to study the dynamics when the island size is larger than the linear layer but smaller than the macroscopic (equilibrium) scale length.
- When the instability parameter Δ' is large and global convection cells develop the process *does not follow the standard Sweet-Parker scenario*^{8,9}. Rather, the reconnection rate *accelerates* when the island size exceeds the skin depth ($d < \lambda < L_x$).
- Physically, the *acceleration is caused by of the intensification of the electromagnetic torque* $\oint_C \mathbf{J} \times \mathbf{B} \cdot d\mathbf{l} = \oint_C \mathbf{J} d\psi$ as the system enters the nonlinear regime. This torque is mainly contributed by the average $J_z B_x$ force between the X- and O-points within a magnetic island.
- *The formation of a narrow scale length* less than the skin depth (already noted by Wesson⁷ and by Drake&Kleva¹¹) is due to the *combined effect of the conservation law* and of the *flow pattern* around the X-point.
- Eventually, the reconnection rate slows down only when the magnetic island width approaches the dimension of the system ($\lambda \approx L_x$).
- One expects that the current spike will be eventually limited by effects not taken into account in the present model like collisions, 3D geometry and possibly secondary instabilities. Further work needs to be done to determine the relevant ones for the interesting applications.
- The present analysis opens the possibility to understand the rapidity of the relaxation phenomena observed in low collisionality plasmas.

REFERENCES

- [1] V.M.Vasyliunas, Rev. Geophys. Space Phys. 13, 303 (1975).
- [2] A.W.Edwards et al, Phys. Rev. Lett. 57, 210 (1986).
- [3] F.Porcelli, Phys. Rev. Lett. 66, 425 (1991).
- [4] H.L.Berk, S.M.Mahajan and Y.Z.Zhang, Phys.Fluids B3, 351 (1991).
- [5] B.Coppi and P.Detragiache, Phys. Lett. A168, 59 (1992).
- [6] L.E.Zakharov and B.Rogers, Phys. Fluids B4, 3285 (1992).
- [7] J.Wesson, Nuclear Fusion 30, 2545 (1990).
- [8] P.A.Sweet, in *Electromagnetic Phenomena in Cosmic Physics*, ed. by B.Lehnert (Cambridge University Press, 1958), p. 123.
- [9] E.N.Parker, J. Geophys. Research 62, 509 (1957).
- [10] B.B.Kadomtsev, Fiz. Plasmy 1, 710 (1975) [Sov. J. Plasma Phys. 1, 389 (1975)].
- [11] J.F.Drake and R.G.Kleva, Phys. Rev. Lett. 66, 1458 (1991).
- [12] S.A.Orszag and G.S.Patterson, Phys. Rev. Lett. 28, 76 (1972).

APPENDIX.

A1) Solution: $\psi(x,y,t) \approx \frac{1}{2} \int_{-\infty}^{\infty} e^{-|\hat{x}-\hat{x}'|} F(\hat{x}',y,t) d\hat{x}'$, where $\hat{x} \equiv x/d$, which shows that ψ has an integral structure such that any fine scale variation of F is smoothed out over a distance $\sim d$.

A2) The manipulation of Eq. (8) involves the neglect of subdominant terms. In the r.h.s. we neglect corrections $O(k^2d)$ contributed by $\partial_y^2\phi$. Exploiting the reflection symmetry with respect to $x = L_x/2$, $y = L_y/2$, the second integral in Eq. (8) can be written as

$$\oint_C J d\psi = -2 \int_0^{L_y} dy (J \partial_y \psi)_{x=0} - 2 \int_0^{L_x} dx [(\partial_y^2 \psi)(\partial_x \psi)]_{y=0}$$

The first integral at the right hand side can be evaluated exactly to yield the r.h.s. of Eq. (10).

The second integral gives a contribution of order $k^2\lambda$, which is negligible when $\Delta'd \sim 8d/\pi k^2 > 1$, and which is significant only in the linear phase when $\Delta'd \sim 1$.